



# In Vitro Antimicrobial Activity and Metal Ion Sensing by Green Synthesized Silver Nanoparticles from Fruits of *Opuntia Ficus Indica* Grown in the Abha Region, Saudi Arabia

Abul Kalam<sup>1,2</sup> · Abdullah G. Al-Sehemi<sup>1,2</sup> · Sulaiman A. Alrumman<sup>3</sup> · Mohammed A. Assiri<sup>1</sup> · Mahmoud F. Moustafa<sup>3,4</sup> · Mehboobali Pannipara<sup>1</sup>

Received: 1 March 2018 / Accepted: 17 May 2018 / Published online: 4 June 2018  
© King Fahd University of Petroleum & Minerals 2018

## Abstract

We developed a green, inexpensive and simple method for the synthesis of silver nanoparticles from the *Opuntia Ficus* (OF) *Indica* fruit juice. The synthesized AgNPs were used as sensor for the detection of toxic metal ( $\text{Hg}^{2+}$ ) using colorimetric technique as well as to investigate the antimicrobial activities against number of clinical isolates of human microbes. The synthesized AgNPs nanoparticles were characterized using UV–Vis spectroscopy, FTIR spectroscopy, scanning electron microscopy and EDX methods. The green synthesized AgNPs showed surface plasmon resonance absorption band at 441 nm, which confirm the formation of AgNPs that were also established by FTIR and EDX analyses. The colour of AgNPs changes from blood red to white in the presence of  $\text{Hg}^{2+}$  only, which can be differentiated and detected by the naked eye within few seconds without the prerequisite of surface amendment from other metals (Co, Ni, Fe, Mn, Pb, Zn, Cr). A good linear response ( $R^2 = 0.97$ ) was obtained towards  $\text{Hg}^{2+}$  ions in the concentration range of  $10^{-3}$  to  $10^{-8}$  M. In addition, all growth of the tested microbial stains ceased in varied range. OFAg-2 had the highest inhibition effect followed by OFAg-1, while OF did not show any antimicrobial activities. *Candida albican* and *Klebsiella pneumonia* are the most susceptible microbes by OFAg-2 and OFAg-1 respectfully. *Klebsiella oxytocam*, *Proteus mirabilis* and *Klebsiella oxytoca* had the moderate susceptibility from OFAg-2 and OF, while *Staphylococcus aureus* was found to be the lowest susceptible microbes. Therefore, OFAg-2 and OFAg-1 probably could be promising pharmaceutical agents against many microbial strains.

**Keywords** Silver nanoparticle · Green synthesis · Sensor · Antimicrobial · Electron microscopy

## 1 Introduction

Weeds plant in Abha area, Saudi Arabia, grown at over 2700 m above sea level is considered a wealth for humanity as it contains many novel compounds that showed antimicrobial activities against multidrug resistant microbes. The detection

of heavy metals in the biological and environmental samples using fast, simple and inexpensive method is still needed for all over the world [1]. It is well known that high concentration of heavy metal ions can cause different kinds of diseases because they form free radicals, which transform DNA bases, augment lipid peroxidation and amend calcium and sulphhydryl homoeostasis [2]. Among various heavy metal ions,  $\text{Hg}^{2+}$  ion is one of the most carcinogenic metal due to its volatile nature and source of various toxicological effects like nephrosis, neurological disorder and innumerable perceptible disorders even at trace concentration also [3]. Therefore, mercury is an extensive environmental toxin that causes unadorned hostile health effects in the human body. Currently, conventional techniques such as atomic absorption spectrometry (AAS) [4], inductively coupled plasma mass spectroscopy (ICP-MS) [5], cold vapour atomic fluorescence spectroscopy (CVAFS) [6], electrochemical method [7], anodic stripping voltammetry [8], atomic force microscopy

✉ Abul Kalam  
abul\_k33@yahoo.com

<sup>1</sup> Department of Chemistry, Faculty of Science, King Khalid University, P.O. Box 9004, Abha 61413, Saudi Arabia

<sup>2</sup> Research Center for Advanced Materials Science (RCAMS), King Khalid University, P.O. Box 9004, Abha 61413, Saudi Arabia

<sup>3</sup> Department of Biology, Faculty of Science, King Khalid University, P.O. Box 9004, Abha 61413, Saudi Arabia

<sup>4</sup> Department of Botany, Faculty of Science, South Valley University, Qena, Egypt



[9], surface plasmon resonance [10], quartz crystal microbalance (QCM) [11], magnetic resonance imaging [12] and surface-enhanced Raman scattering [13] have been used for the detection of  $\text{Hg}^{2+}$  ion level in the environment and humans. The methods mentioned are magnificently used for the detection of  $\text{Hg}^{2+}$  ion and extremely selective and sensitive. Apart from the mentioned advantages, they have some disadvantages like expensive instruments, time and sample preparation, which edge the routine monitoring of  $\text{Hg}^{2+}$  ion. Therefore, there is a great challenge for researchers to establish a simple and cost-effective method for the detection of  $\text{Hg}^{2+}$  ion from the environmental samples. Currently, green synthesized silver nanoparticles (AgNPs) have gained copious additional momentum in the area of sensor and antimicrobial activities due to its low cost synthesis, high extinction coefficient as compared to the AuNPs [14–17]. In our knowledge, it is the first of its kind research on the synthesis of AgNPs using juice of OF fruit at room temperature. Herein, in incessant of earlier works, we have used juice of OF fruit for the synthesis of functionalized AgNPs and corroborate the competency to sense heavy metal ion ( $\text{Hg}^{2+}$ ) in aqueous solution and to investigate the antimicrobial activities against number of clinical isolates of human microbes. We selected this particular fruit as it is easily available in KSA, acts as green catalyst, bioreductant, solvent and might possess sensory properties.

## 2 Materials and Methods

### 2.1 Materials

Silver nitrate ( $\text{AgNO}_3$ ) (BDH reagent,  $\geq 99.0\%$ ) was purchased from Sigma-Aldrich and used as received. The fruits of *Opuntia Ficus (OF) Indica* were collected from the local farmhouse located in Abha near King Khalid University, Kingdom of Saudi Arabia. We used double distilled water for the washing and extracted juice kept in bottle for further use. All isolates were obtained from Biology Department, Faculty of Science and Microbiology Laboratory, Faculty of Medicine, King Khalid University, Saudi Arabia.

### 2.2 Extraction and Synthesis of AgNPs

The fruit juices were filtered through Whatman filter paper and finally centrifuged to remove any solid particles at 40,000 rpm for 5 minutes. Inset of Fig. 1 represents the colour of fruit juice stored in fridge for future use. Different volumes (1, 2 ml) of OF juice were added drop-wise to the conical flasks containing 10 ml of 0.1 molar silver nitrate solutions. All two conical flasks were stirred at room temperature. The solution of colour becomes dark green within 20 minutes but at the end it becomes blood red colour after 1 h and the samples

were assigned as OFAg-1 and OFAg-2, which is the clear indication for the formation of silver nanoparticles (inset of Fig. 1). The green synthesized Ag nanoparticles were stored under cold for further study.

### 2.3 Colorimetric Sensing Properties of AgNPs

The prepared AgNPs were assessed as a colorimetric sensor for numerous metal ions by metal salts solutions ( $10^{-3}$  M) into a dilute solution of green synthesized AgNPs (OFAg-2) (final volume 10 ml) which displayed selective decolorization for  $\text{Hg}^{2+}$  ion only (Fig. 4). We added different concentrations of  $\text{Hg}^{2+}$  ion solution to the solution containing 0.1 ml OFAg-2 in a 10 ml volumetric flask for colorimetric sensing of  $\text{Hg}^{2+}$  ion. The spectral measurements were recorded by using UV–visible spectrophotometer after completion of the reaction.

### 2.4 Solvents Extractions for Antimicrobial Activity

#### 2.4.1 Pathogenic Strains Preparation

Number of clinical isolates to human including five gram-negative bacterial strains *Viz, Shigella flexneri, Klebsiella oxytoca, Klebsiella pneumonia, Pseudomonas aeruginosa* and *Proteus mirabilis*, two gram-positive bacterial strains, *Staphylococcus aureus* and *Micrococcus luteus* and *Candida albicans* were first grown in nutrient broth (NB) and incubated at  $30^\circ\text{C}$  for 24 h for all bacterial isolates and for 49 h for *C. Albicans* [18–20]. All isolates were obtained from Biology Department, Faculty of Science and Microbiology Laboratory, Faculty of Medicine, King Khalid University, Saudi Arabia.

### 2.5 In Vitro Antimicrobial Assay

Examinations of the antimicrobial inhibition activity of OF, OFAg-1 and OFAg-2 were accomplished by using the agar well-diffusion method [19,20]. OF, OFAg-1 and OFAg-2 were examined for their antimicrobial against *M. luteus*, *K. oxytoca*, *S. aureus*, *P. aeruginosa*, *K. pneumonia*, *S. flexneri*, *P. mirabilis* and *Candida albicans*. About 20 millilitres from sterilized nutrient agar medium was poured into sterilized petri dishes and kept at  $24^\circ\text{C}$  till solidification of media. Sterilized petri dishes were inoculated with microbial strains using a sterile loop. Three well of 6 mm in diameter in each plate was made in the solidified agar media by sterile cork-borer then filled with 100  $\mu\text{l}$  from OF, OFAg-1 and OFAg-2. Inoculated plates were kept for about one hour at  $24^\circ\text{C}$  and then incubated at  $29^\circ\text{C}$ . 100  $\mu\text{l}$  of dimethyl sulphoxide (DMSO) was used as a negative control, while synthetic cefoxitin (30  $\mu\text{g}$ ) as positive controls. The experiments were done three times, and the inhibition activities

zones formed on the media were measured with a transparent ruler.

### 3 Characterizations

Ultraviolet–visible (UV–Vis) spectrophotometer (PG instrument) was used to record the absorption spectra of prepared AgNPs, and the progress of reactions was also monitored by its colour change with bare eye. The images of AgNPs were obtained using scanning electron microscopy (SEM; Hitachi S4800) equipped with an energy-dispersive X-ray spectroscopy. Fourier transform infrared (FTIR) spectra were recorded on JASCO 460 plus at room temperature in the range of 4000–500  $\text{cm}^{-1}$ . Raw data of antimicrobial effect of OF, OFAg-1 and OFAg-2 against tested pathogens were analysed and compared by one-way ANOVA in SPSS Statistics.

### 4 Results and Discussion

In the current work, we used juice of OF fruit as bioreducing and capping agent for the synthesis of functionalized AgNPs. The colour of silver ion solution becomes like dark blood after 1 h of addition of fruit juice. This indicates a naked eye confirmation of the formation of AgNPs with the addition of fruit juice (inset Fig. 1). The spectra presented in Fig. 1 shows the monitoring progress of reaction by measuring the UV–Vis spectra of green synthesized AgNPs and pure juice. The existence of sharp and broad surface plasmon resonance (SPR) peak at 441 nm indicates the formation of AgNPs (OFAg-2) [21]. It has been suggested that the shape and position of SPR bands were applied for the estimation

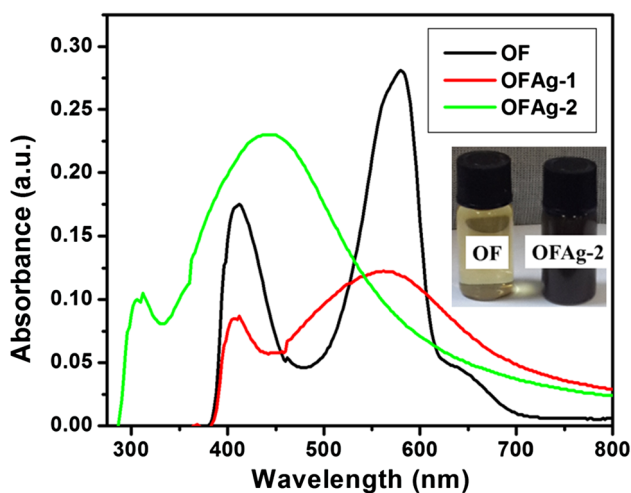


**Fig. 1** UV–visible spectra of fruit juice and prepared silver nanoparticles (OFAg-1 & OFAg-2) and inset shows the images of fruit juice and OFAg-2

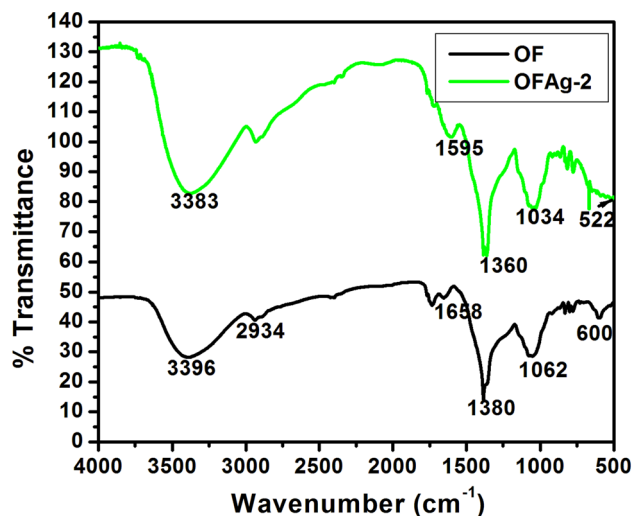


**Fig. 2** FTIR spectra of fruit juice (OF) and prepared silver nanoparticles (OFAg-2)

of optical performances of green synthesized AgNPs. It is clear from the spectra that the absorbance intensity of SPR peak increased, which indicates that the formation of AgNPs can be enhanced by increasing the volume of bioextract due to presence of more bioreducing agent in the fruit juice. The position of SPR band was blueshifted from 562 nm as the volume of juice increases which indicates the shortening of particle size. This change in the optical property is due to excitation of SPR band or interionic fascination of the functional group with the AgNPs. The result revealed that the 2 ml of fruit juice is appropriate for the synthesis of silver nanoparticle.

FTIR used to study the changes detected in the functional group of fruit juice before and after addition to the solution of  $\text{AgNO}_3$ , which are responsible for the reduction, capping and stabilization of AgNPs. The FTIR spectra of prepared silver nanoparticles (OFAg-2) and juices are shown in Fig. 2. The bands appeared in Fig. 2 represent the functional groups of various compounds such as phenol, tannin, flavonoids, alkaloids which are the main components of fruit juice. The band appeared in the 3383–3396  $\text{cm}^{-1}$  region corresponds to the stretching vibration of hydroxyl group of phenolic and alcoholic compounds. The band 3383  $\text{cm}^{-1}$  of OFAg-2 becomes narrow and shifted as compared to the pure juice, which showed the reduction of silver ions into nanoparticles [22]. The band appearance in the 1595–1668  $\text{cm}^{-1}$  region is ascribed to amide-I and C=O stretching vibration of carboxylate group or C=C bond stretching of aromatic groups present in the juice [23]. The band appearance in the 1034–1062  $\text{cm}^{-1}$  region might be due to C–OH stretching vibration of carboxylic acids and alcoholic groups [24]. Besides, the bands at 2933 and 2934  $\text{cm}^{-1}$  are accompanying to C–H deforming vibration. A strong and sharp peak at 1380  $\text{cm}^{-1}$

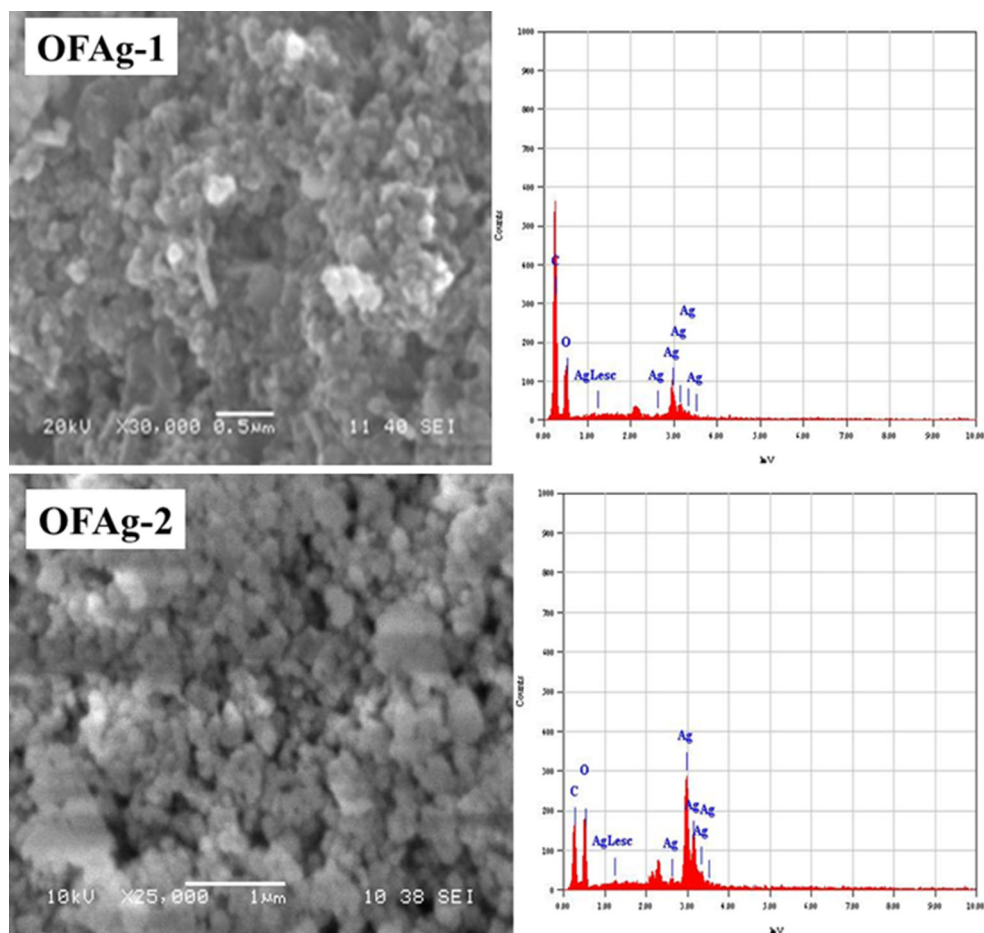


**Fig. 3** SEM images of OFAg-1 and OFAg-2 and corresponding EDX

for fruit juice which shifted to  $1360\text{ cm}^{-1}$  after the bioreduction of silver nanoparticles correspond to the C=C stretching mode of aromatic like flavonoid [22,25]. This investigation also ratifies the presence of organic molecule on the surface of AgNPs which act as capping agent to preclude agglomeration and enhance the stability.

Figure 3a, b displays the scanning electron microscope (SEM) images of as-synthesized AgNPs using different volume (1, 2 ml) of OF fruit juice. It is very clear from the SEM images that the size of prepared silver nanoparticles has been increased by increasing the volume of OF fruit juice. Sample OFAg-1 consists of high degree of agglomeration, whereas OFAg-2 showed small degree of agglomeration; this could be seen in SEM observations that may be due to the effect of bioextract during synthesis. The size of the silver nanoparticles was obtained in the range of 140–153 and 90–103 nm for OFAg-1 and OFAg-2, respectively. Moreover, a SEM/ EDX analysis used to confirm the element present in the synthesized materials (OFAg-2) and the result showed the existence of AgNPs and the amount was 11.99%. The peaks detected around 2.6 keV, 3 keV and 3.20 keV can be consigned to binding energy of OFAg-1 and OFAg-2, respectively [10].

This study clearly reveals that the bioorganic present in the extract perform a significant role in producing the spherical and size-controlled AgNPs materials.

The optical response of various metal ions ( $\text{Cd}^{2+}$ ,  $\text{Zn}^{2+}$ ,  $\text{Co}^{2+}$ ,  $\text{Cu}^{2+}$ ,  $\text{Sr}^{2+}$ ,  $\text{Pb}^{2+}$ ,  $\text{Ni}^{2+}$ ,  $\text{Mn}^{2+}$ ,  $\text{Hg}^{2+}$ ) with concentration of  $10^{-3}\text{ M}$  are shown in Fig. 4. The colour of OFAg-2 becomes white with  $\text{Hg}^{2+}$  solution which represented the selective sensor for  $\text{Hg}^{2+}$  ion (Fig. 4 inset) and SPR peak at 441 nm almost vanishes. It is clearly evident that the absorbance intensity of  $\text{Hg}^{2+}$  had lowest intensity as compared to the rest metal ions. The results revealed that the OFAg-2 nanoparticles can be used for the selective sensing of  $\text{Hg}^{2+}$  ion. Figure 5 represents the optical response of  $\text{Hg}^{2+}$  ion with the concentration ranges from  $10^{-3} - 10^{-8}\text{ M}$ , and the corresponding changes of colour and SPR band were observed. The colour of AgNPs progressively changes to white on increasing the concentration of  $\text{Hg}^{2+}$  ion (inset Fig. 5). The capping agent present on the surface of AgNPs assists the binding of Hg on to the surface of AgNPs, and  $\text{Hg}^{2+}$  is reduced to Hg (0) while Ag (0) oxidized to  $\text{Ag}^+$  ion [26]. According to the electrochemical series, metals with higher electrochemical reduction poten-

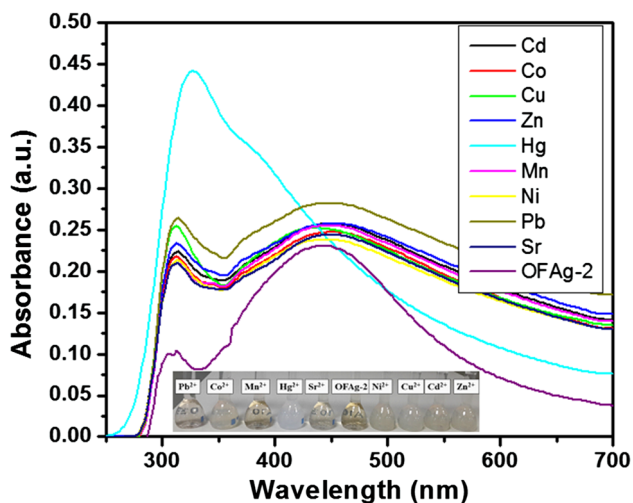


Fig. 4 UV-visible spectra of OFAg-2 with different metal ions ( $10^{-3}$  M) and inset show the images of selective sensing of  $Hg^{2+}$  ion

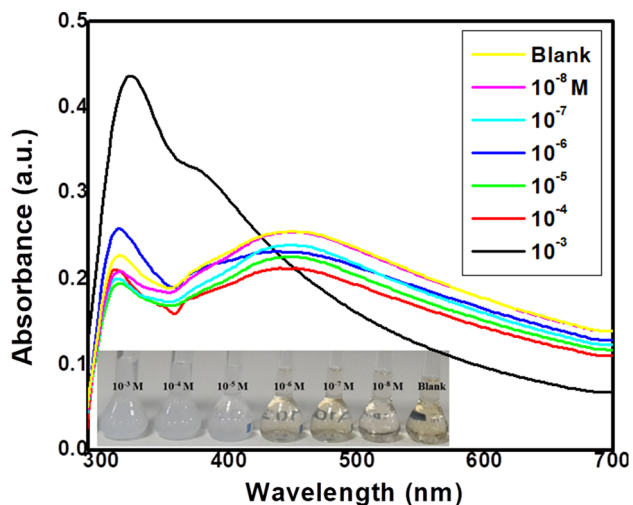


Fig. 5 UV-visible spectra of OFAg-2 with different concentration of  $Hg^{2+}$  ( $10^{-3}$  M to  $10^{-8}$  M) and inset shows images of colour variations with different concentration of  $Hg^{2+}$

tial act as better oxidizing agents ( $Ag^+$  is 0.80 V whereas for  $Hg^{2+}$  is 0.92 V). Further, Ag-Hg nano-alloy formation takes place due to reaction of  $Ag^+$  ion with  $Hg^{2+}$  ion [27]. Many reports are available concerning the use of AgNPs as sensor by the surface modification using other molecules. But in the current research, we used as-synthesized AgNPs without surface modification. The spectra result shows that by increasing the concentration of  $Hg^{2+}$  ion absorption intensity decreases simultaneously and redshift in SPR peak position. The regression analysis recommended good linearity of the established optical sensor with regression coefficient ( $R^2$ ) of 0.97.

Table 1 Antimicrobial activities of OF, OFAg-1 and OFAg-2

Chemicals name	Strain name	<i>M. luteus</i>	<i>K. oxytoca</i>	<i>P. mirabilis</i>	<i>C. albicans</i>	<i>S. flexneri</i>	<i>P. aeruginosam</i>	<i>K. pneumonia</i>
OF	<i>S. aureus</i>	NI	NI	NI	NI	NI	NI	NI
OFAg-1	<i>S. aureus</i>	1.37 ± 0.15	1.57 ± 0.11	2.47 ± 0.15	2.80 ± 0.10	2.43 ± 0.05	2.37 ± 0.32	2.50 ± 0.11
OFAg-2	<i>S. aureus</i>	2.33 ± 0.15	2.63 ± 0.25	2.93 ± 0.05	3.47 ± 0.15	3.50 ± 0.11	3.60 ± 0.11	3.43 ± 0.05
(Cefoxitin-30 µg)	<i>S. aureus</i>	2.77 ± 0.34	3.32 ± 0.18	2.32 ± 0.16	2.97 ± 0.18	2.83 ± 0.16	2.88 ± 0.31	2.78 ± 0.41

NI, no inhibition activities; (Cefoxitin-30 µg); positive control

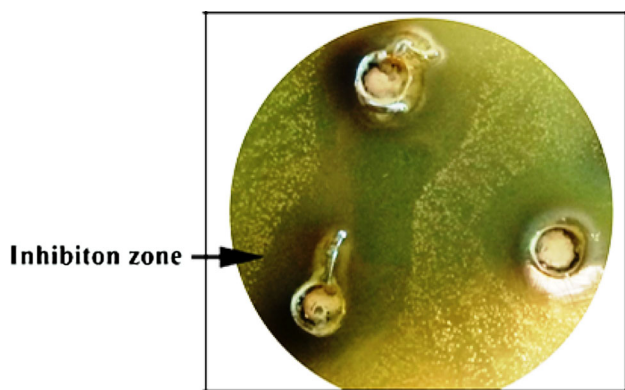


Fig. 6 Inhibition activities of OFAg-2 against *S. aureus*

## 5 Inhibitory Properties of OF, OFAg-1 and OFAg-2

Table 1 shows the inhibition activities of OF, OFAg-1 and OFAg-2 obtained against a range of human pathogenic microbes. The results showed that OFAg-1 and OFAg-2 could affect 100% of the tested panel of microbial species while OF had no inhibition activities. It is apparent in this research that OFAg-2 is more potent than OFAg-1 against all tested microbes. In the form of zone of inhibition *Candida albican* and *Klebsiella pneumonia* are the most susceptible microbes by OFAg-2 and OFAg-1 in the range between ( $3.46 \pm 0.15$  mm to  $3.43 \pm 0.05$  mm) and ( $2.43 \pm 0.05$  mm to  $2.50 \pm 0.05$  mm). *Klebsiella oxytoca*, *Proteus mirabilis* and *Klebsiella oxytoca* had the moderate inhibitory activity from OFAg-2 and OF while in the range between ( $1.57 \pm 0.11$  mm and  $2.90 \pm 0.11$  mm). *Staphylococcus aureus* were found to be the lowest susceptible microbes with inhibition zone in the range between ( $1.37 \pm 0.15$  mm to  $2.33 \pm 0.15$  mm) (Fig. 6). Cefoxitin ( $30 \mu\text{g}$ ) showed inhibition activity against all tested human pathogenic in the range between ( $2.77 \pm 0.34$  mm and  $3.32 \pm 0.18$  mm) while dimethyl sulphoxide (DMSO) did not exhibit any activities. Recently, we reported the effects of green synthesized AgNPs against seven pathogenic bacteria [15]. The results indicated that the antimicrobial activity depends on the size of AgNPs. The current results are also persistent with the earlier results in contrast to extensive variety of gram-positive and gram-negative bacterial pathogens [28–30].

## 6 Conclusion

We established the biosynthesis of AgNPs using juice of *Opuntia Ficus Indica* fruit that is advantageous, inexpensive and eco-friendly. The UV–visible spectra obtained at 441 nm and colour changes confirms the formation of AgNPs. The functional groups present in the fruit juice and silver

nanoparticles were confirmed using FTIR studies, which are responsible for the reduction and capping of silver. The SEM images of prepared AgNPs showed spherical shape and size ranges between 90 and 140 nm. The synthesized AgNPs used were as sensor for the detection of toxic metal ( $\text{Hg}^{2+}$ ) using colorimetric technique as well as to investigate the antimicrobial activities against number of clinical isolates of human microbes. A good linear response ( $R^2 = 0.97$ ) was obtained towards  $\text{Hg}^{2+}$  in the concentration range of  $10^{-3}$  to  $10^{-8}$  M. In addition, all possible growth of the tested microbial stains ceased in varied range. OFAg-2 had the highest inhibition effect followed by OFAg-1, while OF did not show any antimicrobial activities. Therefore, OFAg-2 and OFAg-1 probably could be promising pharmaceutical agents against many microbial strains.

**Acknowledgements** Authors are thankful to the Dean Scientific Research and Research Center for Advanced Materials Science (RCAMS), King Khalid University, Abha, Saudi Arabia, for the technical and administrative support. We are also thankful to the Head of Department, Chemistry, College of Science, King Khalid University, Abha, Saudi Arabia, for providing facilities to carry out the research work.

## References

- Martinez, A.W.; Phillips, S.T.; Carrilho, E.; Thomas, S.W.; Sindi, H.; Whitesides, G.M.: Simple telemedicine for developing regions: camera phones and paper-based microfluidic devices for real-time. *Off Site Diagn. Anal. Chem.* **80**, 3699–3707 (2008)
- Valko, M.; Morris, H.; Cronin, M.T.: Metals: toxicity and oxidative stress. *Curr. Med. Chem.* **12**, 1161–1208 (2005)
- Harris, H.H.; Pickering, I.J.; George, G.N.: The chemical form of mercury in fish. *Science* **301**, 1203 (2003)
- Cizdziel, J.V.; Gerstenberger, S.: Determination of total mercury in human hair and animal fur by combustion atomic absorption spectrometry. *Talanta* **64**, 918–921 (2004)
- Kenduzler, E.; Ates, M.; Arslan, Z.; McHenry, M.; Tchounwou, P.B.: Determination of mercury in fish otoliths by cold vapor generation inductively coupled plasma mass spectrometry (CVG-ICP-MS). *Talanta* **93**, 404–410 (2012)
- Geng, W.; Nakajima, T.; Takanashi, H.; Ohki, A.: Determination of mercury in ash and soil samples by oxygen flask combustion method-cold vapor atomic fluorescence spectrometry (CVAFS). *J. Hazard. Mater.* **154**, 325–330 (2008)
- Yang, Y.Q.; Kang, M.M.; Fang, S.M.; Wang, M.H.; He, L.H.; Zhao, J.H.; Zhang, H.Z.; Zhang, Z.H.: Electrochemical biosensor based on three-dimensional reduced graphene oxide and polyaniline nanocomposite for selective detection of mercury ions. *Sens. Actuators B* **214**, 63–69 (2015)
- Ugo, P.; Moretto, L.M.; Mazzocchin, G.A.: Voltammetric determination of trace mercury in chloride media at glassy carbon electrodes modified with polycationic ionomers. *Anal. Chim. Acta* **305**, 74–82 (1995)
- Zhang, T.; Cheng, Z.G.; Wang, Y.B.; Li, Z.G.; Wang, C.X.; Li, Y.B.; Fang, Y.: Self-assembled 1-octadecanethiol monolayers on graphene for mercury detection. *Nano Lett.* **10**, 4738–4741 (2010)
- Zhang, H.Y.; Yang, L.Q.; Zhou, B.J.; Liu, W.M.; Ge, J.E.C.; Wu, J.S.; Wang, Y.; Wang, P.F.: Ultrasensitive and selective gold film-based detection of mercury (II) in tap water using a laser scanning



- confocal imaging-surface plasmon resonance system in real time. *Biosens. Bioelectron.* **47**, 391–395 (2013)
11. Wang, M.H.; Liu, S.L.; Zhang, Y.C.; Yang, Y.Q.; Shi, Y.; He, L.H.; Fang, S.M.; Zhang, Z.H.: Graphene nanostructures with plasma polymerized allylamine biosensor for selective detection of mercury ions. *Sens. Actuators B* **203**, 497–503 (2014)
  12. Liang, G.H.; Zhang, P.; Li, H.X.; Zhang, Z.Y.; Chen, H.; Zhang, S.; Kong, J.L.: An efficient strategy for unmodified nucleotide-mediated dispersion of magnetic nanoparticles, leading to a highly sensitive MRI-based mercury ion assay. *Anal. Chim. Acta* **726**, 73–78 (2012)
  13. Xu, L.G.; Yin, H.H.; Ma, W.; Kuang, H.; Wang, L.B.; Xu, C.L.: Ultrasensitive SERS detection of mercury based on the assembled gold nanochains. *Biosens. Bioelectron.* **67**, 472–476 (2015)
  14. Jiang, X.C.; Yu, A.B.: Silver nanoplates: a highly sensitive material toward inorganic anions. *Langmuir* **24**, 4300–4309 (2008)
  15. Kalam, A.; Al-Sehemi, A.G.; Alrumman, S.; Du, G.; Pannipara, M.; Assiri, M.; Almalki, H.; Moustafa, M.F.: Colorimetric sensing of toxic metal and antibacterial studies by using bioextract synthesized silver nanoparticles. *J. Fluoresc.* **27**, 2045–2050 (2017)
  16. Ali, S.G.; Ansari, M.A.; Khan, H.M.; Jalal, M.; Mahdi, A.A.; Cameotra, S.S.: Antibacterial and antibiofilm potential of green synthesized silver nanoparticles against imipenem resistant clinical isolates of *P. aeruginosa*. *BioNanoScience* (2018). <https://doi.org/10.1007/s12668-018-0505-8>
  17. Jalal, M.; Ansari, M.A.; Ali, S.G.; Khan, H.M.; Eldaif, W.A.H.; Alrumman, S.A.: Green synthesis of silver nanoparticles using leaf extract of *Cinnamomum tamala* and its antimicrobial activity against clinical isolates of bacteria and fungi. *Int. J. Adv. Res.* **4**(12), 428–440 (2016)
  18. Moustafa, M.F.; Alrumman, S.A.: First report about pharmaceutical properties and phytochemical analysis of *Rosa abyssinica* R. Br. ex Lindl. (Rosaceae). *Pak. J. Pharm. Sci.* **28**(6), 2009–17 (2015)
  19. Alrumman, S.A.: Phytochemical and antimicrobial properties of *Tamarix aphylla* L. leaves growing naturally in the Abha Region, Saudi Arabia. *Arab. J. Sci. Eng.* **41**(6), 2123–2129 (2016)
  20. Alrumman, S.A.: In vitro antimicrobial activity and GC-MS findings of the Gel of *Aloe Vacillans* Forssk. of Abha Region, Saudi Arabia. *Arab. J. Sci. Eng.* **43**(1), 155–162 (2018)
  21. Vellaichamy, B.; Periakaruppan, P.: Green synthesized nanospherical silver for selective and sensitive sensing of  $\text{Cd}^{2+}$  colorimetrically. *RSC Adv.* **6**, 35778 (2016)
  22. Jacob, S.J.P.; Prasad, V.L.S.; Sivasankar, S.; Muralidharan, P.: Biosynthesis of silver nanoparticles using dried fruit extract of *Ficus carica*—screening for its anticancer activity and toxicity in animal models. *Food Chem. Toxicol.* **109**, 951–956 (2017)
  23. Konsolakis, M.; Kaklidis, N.; Marnellos, G.E.; Zaharaki, D.; Komnitsas, K.: Assessment of biochar as feedstock in a direct carbon solid oxide fuel cell. *RSC Adv.* **5**, 73399–73409 (2015)
  24. Hashemian, H.; Shayegan, J.: A comparative study of cellulose agricultural wastes (almond shell, pistachio shell, walnut shell, tea waste and orange peel) for adsorption of violet B dye from aqueous solutions. *Orient. J. Chem.* **30**, 2091–2098 (2014)
  25. Kizil, R.; Induraj, J.; Seetharaman, K.: Characterization of irradiated starches by using FT-Raman and FTIR spectroscopy. *J. Agric. Food Chem.* **50**(14), 3912–3918 (2002)
  26. Farhadi, K.; Forough, M.; Molaei, R.; Hajizadeh, S.; Rafipour, A.: Highly selective  $\text{Hg}^{2+}$  colorimetric sensor using green synthesized and unmodified silver nanoparticles. *Sens. Actuators B* **161**, 880–885 (2012)
  27. Bhattacharjee, Y.; Chakraborty, A.: Label-free cysteamine-capped silver nanoparticle-based colorimetric assay for  $\text{Hg(II)}$  detection in water with subnanomolar exactitude. *ACS Sustain. Chem. Eng.* **2**, 2149 (2014)
  28. Rai, M.; Kon, K.; Ingle, A.; Duran, N.; Galdiero, S.; Galdiero, M.: Broad-spectrum bioactivities of silver nanoparticles: the emerging trends and future prospects. *Appl. Microbiol. Biotechnol.* **98**, 1954 (2014)
  29. Galdiero, S.; Falanga, A.; Vitiello, M.; Cantisani, M.; Marra, V.; Galdiero, M.: Silver nanoparticles as potential antiviral agents. *Molecules* **16**, 8894 (2011)
  30. Khamhaengpol, A.; Siri, S.: Green synthesis of silver nanoparticles using tissue extract of weaver ant larvae. *Mater. Lett.* **192**, 72–75 (2017)

